PERGAMON

International Journal of Heat and Mass Transfer 41 (1998) 3005–3013

International Journal of HEAT and MASS TRANSFER

Effect of baffle size, perforation, and orientation on internal heat transfer enhancement

Prashanta Dutta, Sandip Dutta*

Department of Mechanical Engineering, University of South Carolina, Columbia, SC 29208, U.S.A.

Received 17 June 1997; in final form 4 December 1997

Abstract

An experimental investigation of frictional loss and heat transfer behavior of turbulent flow in a rectangular channel with isoflux heating from the upper surface is presented for different sizes, positions, and orientations of inclined baffles attached to the heated surface. Both solid and perforated baffles are used. Inclined perforated baffle combines three major heat transfer techniques, e.g. boundary layer separation, internal flow swirls, and jet impingement. Results indicate that there exists an optimum perforation density to maximize heat transfer coefficients and this optimum perforation exhibits a strong jet impingement technique from the lower confined channel along with other enhancement techniques of heat transfer.

Nomenclature

a, c distances from the start of heating to the start of baffle and to the end of baffle
b gap between baffle and lower surface, channel blockage $\cong 1-b/H$
D, d channel hydraulic diameter and jet hole diameter
f, f_s friction with and without (smooth channel) baffle
H channel height
h heat transfer coefficient
k thermal conductivity of air
L, W, t length, width, and thickness of baffles
M, N number of equispaced holes in longitudinal and transferse directions
Nu local channel centerline Nusselt number: $Nu = hD/k$
Nu_0 Nusselt number for fully developed pipe flow at the same Reynolds number Dittus–Boelter equation: $Nu_0 = 0.02Re^{0.8}$ (Incropera and DeWitt [1])
Nu_{avg} average of channel centerline Nu
Re Reynolds number: $Re = \rho VD/\mu$
T_b, T_w bulk temperature of air and wall temperature
U, V channel centerline and average bulk flow velocities of cooling air, $V = 0.766U$.

Greek symbols
α angle of baffle inclination
μ air viscosity
ρ air density.

1. Introduction

Like jet impingement, ribs, and other heat transfer enhancement techniques, insertion of baffles in heat transfer devices is popular to promote better mixing of the coolant and increase cooling performance. Applications of the inclined baffles may be in the large land based gas turbine blade coolant path, air-cooled solar collectors, heat exchangers, and power plants. The baffle plate is usually attached to the heated surface to augment heat transfer by providing additional area for heat transfer and better mixing. To augment the heat transfer coefficient of gases in internal flow, the following techniques are generally used: (i) Boundary layer disturbance caused by periodically placed ribs on the heat transfer surface. These ribs are small and do not disturb the core flow and therefore, the turbulence enhancement and boundary layer break down are mostly localized near the heat transfer surface. Ribs provide excellent cooling enhancement with a comparatively low penalty in the

* Corresponding author.

0017–9310/98 $19.00
PII: S0017-9310(98)00016-7

pressure drop increase for low to moderate Reynolds numbers. (ii) Impingement cooling uses high velocity jets to cool the surface of interest. However, often a large region needs to be cooled and multiple jets are required. Multiple jets get deflected in the presence of cross flow developed by upstream spent-jets. (iii) The third technique is the use of internal flow swirls or tape twisters. This technique creates a significant amount of bulk flow disturbance, and pressure drop may be higher compared to the increase in heat transfer coefficient.

Inclined solid baffles may be considered as a combination of ribs and channel inserts. The baffles are big enough to disturb the core flow, but like ribs, they are mounted on or near the heat transfer surface and can be periodic in nature. Perforations in inclined baffles create a multiple jet impingement condition and thus create a situation where all three major heat transfer coefficient enhancement techniques work in unison. In the past, experimental results were published with baffle plates perpendicular to the flow direction. Among important studies, Berner et al. [2] obtained mean velocity and turbulence results in flow over baffles; and Habib et al. [3] investigated heat transfer and flow over perpendicular baffles of different heights. But these works mainly emphasized on baffles that were perpendicular to the flow direction and for that reason penalties (friction factor) were higher than the improvements (heat transfer augmentation). Recently, Dutta et al. [4] reported heat transfer enhancement with an inclined perforated baffle.

Perforated baffles use impingement cooling and there are volumes of publications available on multiple jet impingement. Among important contributions, Goldstein and Timmers [5], and Koopman and Sparrow [6] discussed the heat transfer enhancement by multiple jet impingement. Florshuetz et al. [7] presented the heat transfer distribution created by jet array in a cross flow. Lin et al. [8] experimentally showed the heat transfer behaviors of a confined slot impingement. In the present experimental work, impingement holes are drilled on the inclined baffle and since baffles are inclined, these jets are directed toward the heat transfer surface. Note that this jet impingement concept cannot be adopted in a perpendicular baffle arrangement.

Experimental study of Dutta et al. [4] on perforated baffles showed better heat transfer augmentation with perforations compared to that with a solid (not perforated) baffle, if the plate is attached to the heated surface and properly aligned in the direction of the flow. This baffle position was considered as a favorable orientation to enhance the local heat transfer coefficient up to five times of the results obtained in smooth channel. Unlike previous publications, in this paper experimental analysis of heat transfer enhancement is presented with different inclined baffles to achieve optimum perforation and inclination condition. These baffles with different perforation densities are oriented in the favorable direction [4] and the angle of inclination is varied for favorable baffles to search for an optimum angle of inclination.

2. Experimental facility

A not-to-scale schematic of the experimental setup is shown in Fig. 1. The cross-section of the smooth wind-tunnel is 24.92 cm × 4.92 cm that has an aspect ratio of 5. All measurements are done along the centerline of the rectangular channel. Geometrical results are presented in terms of the channel height (H = 4.92 cm), whereas, heat transfer and friction factors are presented in terms of channel hydraulic diameter, D (D = 8.217 cm). A suction mode blower draws air through this rectangular wind-tunnel through an upstream contraction and flow straighteners. This air-flow develops through a $31H$ long unheated entrance and the exit is at a $22.2H$ distance downstream of the heated test section. The heated test section is $19.2H$ long, and is instrumented on the top surface (24.92 cm wide). Commercial fiberglass insulation is used at the exterior to minimize thermal energy leakage. Stainless steel foil heaters are connected to a voltage controller to provide uniform heat flux boundary condition. These foil heaters are aligned perpendicular to the flow direction similar to a configuration used by Han [9]. Forty six isoflux heaters of the same size and shape are mounted on the upper surface of the test section, the other three sides are unheated and properly insulated. Thermocouples are laid along the channel centerline and each strip of the foil heater is equipped with one thermocouple similar to Han [9]. One thermocouple at the inlet and two thermocouples at the outlet measure the inlet and outlet bulk fluid temperatures. Bulk temperatures at all other thermocouple locations are calculated from an energy balance. There are two turbulators, one at the inlet and the other at the outlet, to ensure turbulent boundary layer and good mixing of the bulk flow for bulk temperature measurements. These 7 mm diameter turbulators are located at $1.55H$ upstream and $2.3H$ downstream of the test section. Inlet and outlet thermocouples are located at $0.9H$ upstream and $5.4H$ downstream of the heated test section; and two pressure probes are located $2.45H$ upstream and $4.4H$ downstream of the test section.

Figure 2(a) shows views of a perforated baffle and Fig. 2(b) gives the position of baffle in the test section along with necessary nomenclature. Eight different baffle plates of the same width (W = 24.92 cm) and thickness (t = 0.5 cm) but with different length and perforations are used. Leading edges of these baffles are kept sharp to reduce possible flow disturbance by the protruding edge and drilled holes (perforations) through these baffles create jet impingement effects. Drilled holes are oriented to make impingement jets normal to the heated surface. However, developing length ($0.5d$) of issuing jets in the baffle plates

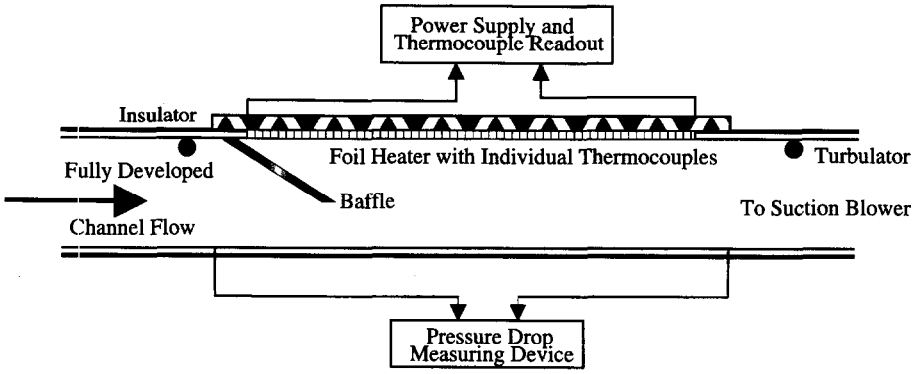

Fig. 1. Schematic diagram of the experimental setup.

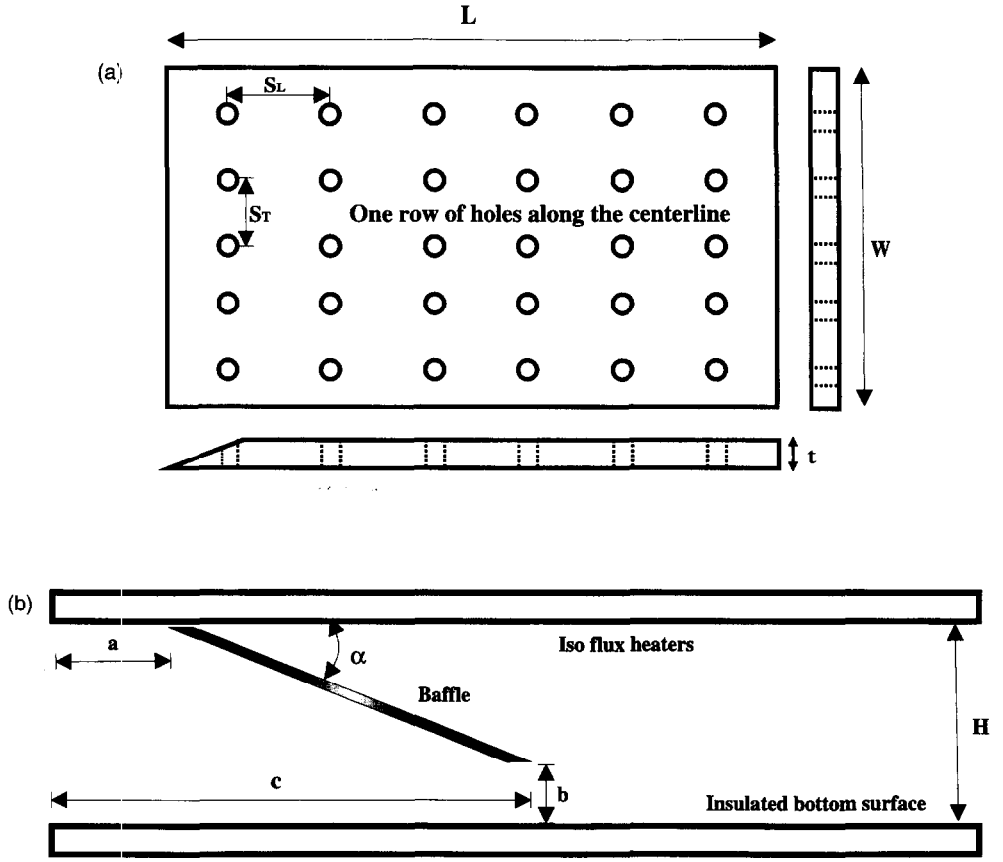

Fig. 2. (a) Baffle plate with associated nomenclature. (b) Position of a baffle in the test section.

may be too short to have any impact on the directionality of the drilled holes. All these perforated baffles have a fixed hole-diameter $d = 1.07$ cm and hole-center to hole-center spacing is varied from baffle to baffle. A row of impingement holes is placed along the centerline of the perforated baffle to match the thermocouple locations.

Table 1 summarizes the geometrical features of baffles. Flow blockage created by baffles varies with plate perforation density and plate orientation. A 3 mm gap between the top heater surface and the baffle is maintained to avoid flow stagnation and burning at the baffle plate contact.

Table 1
Identification of baffles

Baffle No.	Type	Length L/H	Longitudinal pitch of holes S_L/d	Transverse pitch of holes S_T/d	M	N
1	Perforated	5.9	5.9	5.9	4	3
2	Perforated	5.9	3.86	3.86	6	5
3	Perforated	5.9	2.1	2.1	12	11
4	Perforated	2.85	5.9	5.9	3	3
5	Perforated	2.85	3.86	3.86	3	5
6	Perforated	2.85	2.1	2.1	7	11
7	Solid	5.9	No holes	No holes	0	0
8	Solid	2.85	No holes	No holes	0	0

Thermal energy lost is estimated from a separate heat-loss-experiment done on the test facility without air-flow. A heat loss characteristic curve is developed for each thermocouple location. It is found that the maximum local heat flux loss, q''_{loss}, is less than 5% of the total local heat flux supplied, q''. The wall temperatures are measured directly by the embedded thermocouples and the bulk temperatures are estimated from the heat carried by the air stream. The local heat transfer coefficient, h, is obtained from the formula:

$$h = \frac{q'' - q''_{loss}}{T_w - T_b} \tag{1}$$

Channel hydraulic diameter, D, is used to calculate the local Nusselt number, and the average Nu is calculated from the arithmetic average of all local Nusselt numbers.

The friction factor is evaluated from the pressure drop along the channel axis as:

$$f = \frac{\Delta P \cdot D}{\frac{1}{2}\rho L V^2} \tag{2}$$

Where ΔP is the pressure drop across the instrumented test section and L is the length of the test section. Since the pressure taps are located upstream and downstream of the actual test section, a correction on the pressure drop is performed based on the smooth channel analysis. Unlike Dutta et al. [4], the Reynolds number is calculated on the basis of channel average velocity and channel hydraulic diameter. The channel centerline velocity is measured and a relation ($V = 0.766U$) is derived to get the average velocity, V, from centerline velocity, U, by a 1/7th power law velocity profile in a turbulent boundary layer.

2.1. Error analysis

The experimental errors are evaluated by using the standard single sample uncertainty analysis. In this work, the maximum uncertainty occurs in friction factor calculations and that is less than $\pm 7\%$. The maximum error in calculating the flow Reynolds number is estimated to be within $\pm 4\%$; and maximum uncertainties of the measured heat flux and calculated Nusselt numbers are within $\pm 1\%$ and $\pm 5\%$ respectively.

3. Results and discussion

The heat transfer coefficient of gases is low compared to that of liquids. The fundamental objective of this study is to improve the heat transfer behavior of a gaseous fluid in a channel by the placement of inclined perforated baffles and seek a direction towards an optimum performance from these baffles. Eight different baffle plates of different geometries are used and geometrical characteristics of these baffles are listed in Table 1. Figures 3–5

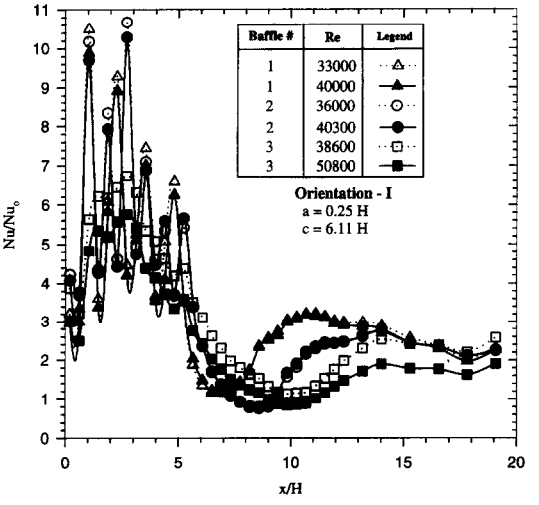

Fig. 3. Local Nusselt number ratio distribution along the channel centerline for Baffle Plates 1, 2 and 3.

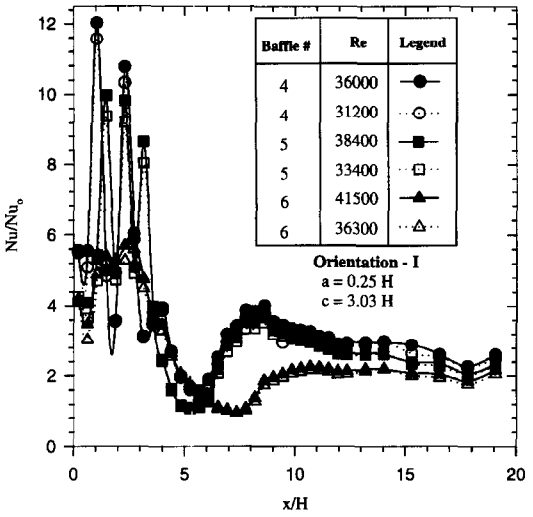

Fig. 4. Local Nusselt number ratio distribution along the channel centerline for Baffle Plates 4, 5, and 6.

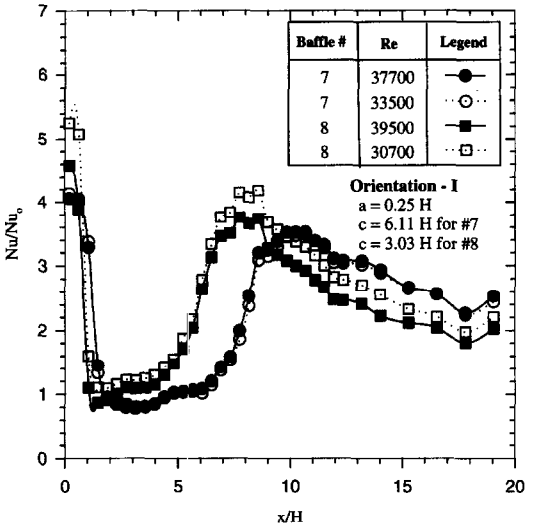

Fig. 5. Local Nusselt number ratio distribution along the channel centerline for Baffle Plates 7 and 8.

show the Nusselt number ratios, Nu/Nu_0, for different baffle plates (different sizes and perforation densities) placed at the same location in the channel. These Nusselt number ratios indicate the amount of improvement in heat transfer coefficient obtained by these baffles over a fully developed smooth channel condition. According to Dutta et al. [4] for this rectangular channel a fully developed heat transfer coefficient in smooth channel condition was achieved at $x/H = 5.0$ downstream from the start of the heater, and the Nusselt number ratio remained within 1.51 to 1.65. A greater than unity Nusselt number ratio for this high aspect ratio channel is supported by the laminar flow results given by Kays and Crawford [10]. Fully developed Nusselt number increases with an increase in the aspect ratio of the channel.

Figure 3 illustrates centerline Nusselt number distribution for Baffles 1, 2 and 3 (see Table 1 for baffle dimensions). The overall dimensions of these three baffles are the same, but perforation densities are different. The local Nusselt number ratio is high at the start of the heating section due to the development of the thermal boundary layer. Dutta et al. [4] reported that at the start of the heated surface, the local Nusselt number ratio varied from 3.16 to 3.85 for this rectangular channel. Baffle insertion at the beginning of the heated section disturbs the boundary layer formation and significant heat transfer coefficient enhancement is noted. Local Nu/Nu_0 peaks are due to the jet impingement effect and these multiple impinging jets develop a highly turbulent cross flow that also enhances the heat transfer coefficient. Near the trailing end of the baffle, jet enhanced turbulent mixing becomes weak due to a divergent orientation of the baffle that results in a decrease of the Nusselt number ratio. The downward trend of Nusselt ratio continues until the end of the baffle. Immediately after the baffle, the heat transfer coefficient increases by the by-passed flow that does not participate in impingement and further downstream the heat transfer behavior approaches a smooth channel condition. An interesting observation is that Nusselt numbers are mostly higher for a plate of less perforation density (Baffle 1). Table 1 indicates that Baffle 1 has a fewer number of holes compared to Baffles 2 and 3, but all plates have same overall dimensions.

An enhancement of heat transfer coefficient obtained by Baffle 1 may be due to the fact that cross flow by spent jets is stronger for more perforated plate and that reduces impingement effect. Moreover, due to higher flow resistance in Baffle 1, more air passes through the gap between the baffle and the bottom surface; and that increases the reattachment heat transfer coefficient. It is interesting to note that the perforation density significantly affects the location of the reattachment heat transfer enhancement. The reattachment zone occurs early in less perforated plate than that of more perforated baffle. It can be argued that flow passing through impingement chamber is stronger in more perforated baffle and as a result the by-pass flow is weaker and thus reattachment is delayed. As mentioned earlier, one thermocouple in each foil heater gives the local wall temperature at channel centerline (location of jet impingement) and therefore, presented results do not reflect span-averaged Nusselt number characteristics.

Figure 4 shows the centerline Nusselt number distribution for Baffles 4, 5, and 6. Like Fig. 3, these baffles have the same overall dimensions, but with different perforation densities. This figure shows a similar Nusselt number ratio distribution as Fig. 3. Since these plates are

small compared to those of Fig. 3, the number of local peaks at the start of the heated section is less. Moreover, the secondary peak (due to reattachment) in local Nusselt number ratio distribution occurs early at the downstream of the baffle and a longer uniform Nusselt number ratio results at downstream due to a shorter region of disturbance. Baffles used in Fig. 4 have more angle of inclination than those of Fig. 3; and this results in a higher momentum to the impingement jets that increases local heat transfer compared to a more streamlined baffle orientation of Fig. 3.

Figure 5 presents the local Nusselt number distribution at the centerline of the channel for Baffles 7 and 8. In this case both plates are solid, i.e. without perforations. These solid plates 7 and 8 resemble the plate dimensions used in Figs. 3 and 4 respectively. It is clear that the heat transfer characteristics of these solid plates is completely different from those of the perforated plates. Figure 5 shows that these baffle plates deflect the bulk flow away from the heated surface, and the peak occurs at the downstream of the baffle due to flow reattachment. Baffle 8 is shorter than 7, and is at a steeper angle of attack. Results indicate that Baffle 8 has a higher Nu/Nu_0 peak, and it occurs at an upstream location compared to that of Baffle 7.

After studying the effect of perforation densities on heat transfer coefficient, local Nusselt number variations along the centerline of the heated target surface are explored for different angular positions of baffles. Figures 6 and 7 show the heat transfer characteristics for Baffle Plates 1 (perforated) and 8 (solid) respectively for different angular positions. These two plates are not selected randomly, but on the basis of their performance described before. Earlier figures indicate that perforated

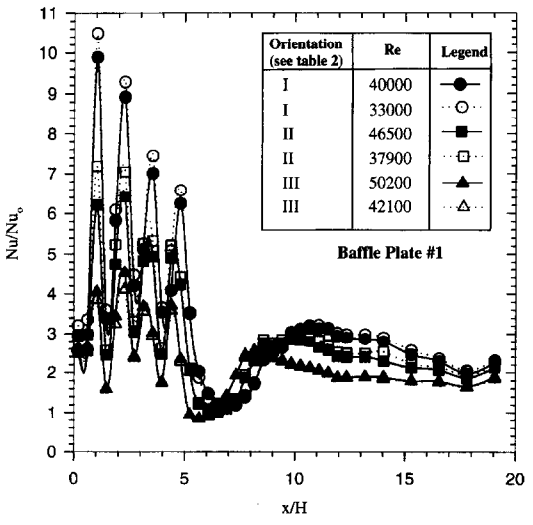

Fig. 6. Local Nusselt number ratio distribution along the channel centerline for Baffle Plate 1 at different angles.

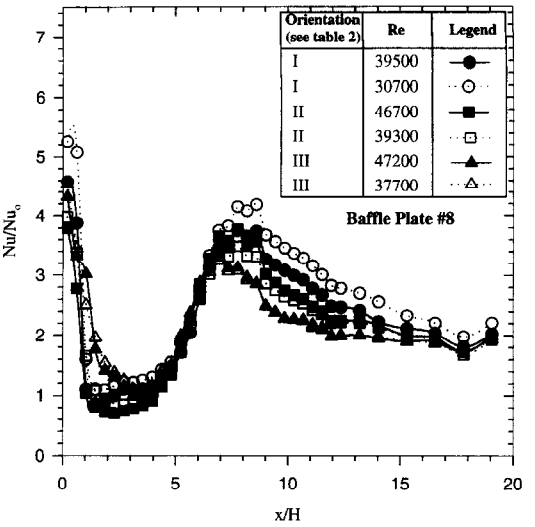

Fig. 7. Local Nusselt number ratio distribution along the channel centerline for Baffle Plate 8 at different angles.

baffle improves heat transfer coefficient compared to a similar dimensioned solid plate for this favorable configuration. It is also observed that the perforated baffles having moderate porosity is better (Figs. 3 and 4) for channel centerline heat transfer than those of densely perforated plates of the same overall dimension. Therefore, Baffle 1 is recommended over Baffles 2 and 3; Baffle 1 is selected for presenting angular variations as a superior heat transfer promoter and Baffle 8 as a worse server in this group of baffles. These different angular positions are considered for each plate. A summary of these plate orientations is given in Table 2. In both figures, the performance of baffle plates deteriorates with the decrease in angle of inclination of the baffle. A higher angle of inclination shows higher Nusselt number ratios in the range of angles studied, and there are two possible explanations for this observation. The first explanation is, as the angle decreases, the plate becomes almost flat and fails to provide jet impingement due to a low-pressure difference across the jet holes; and the second explanation is, in case of a lower angle, a weaker reattachment is expected.

Seyedein et al. [11] numerically investigated the jet-deflection by cross-flow in a converging confinement chamber with different convergent angles of confinement. But the present configurations have a divergent confinement chamber. In a divergent chamber, the flow area increases, therefore, the cross-flow is weaker than a non-divergent channel. However, the distance of the target surface increases from the issuing jet. The advantage of this divergent configuration is its ability to be accommodated in a periodic fashion.

Figures 8 and 9 illustrate the effect of plate position in

Table 2
Orientation of baffles (see Fig. 2 for the length scale nomenclature)

			Long baffles (1, 2, 3, 7)		Short baffles (4, 5, 6, 8)	
Orientation	a/H	b/H	c/H	α	c/H	α
I	0.25	0.39	6.11	6.4°	3.03	9.6°
II	0.25	0.51	6.12	5.0°	3.05	7.7°
III	0.25	0.64	6.13	3.8°	3.07	5.7°

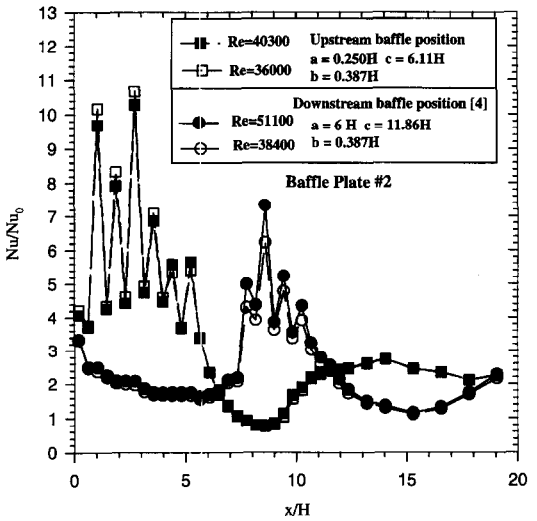

Fig. 8. Comparison of local Nusselt number ratio distribution along the channel centerline for different positions of Baffle 2.

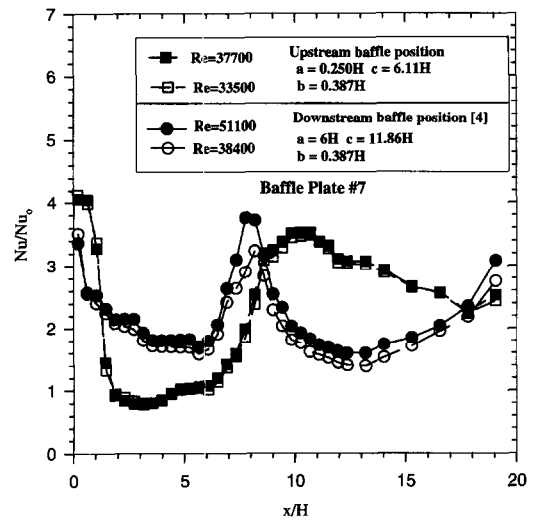

Fig. 9. Comparison of local Nusselt number ratio distribution along the channel centerline for different positions of Baffle 7.

the channel on the local heat transfer distribution for Baffle 2 and Baffle 7 respectively. Two different positions of baffle are presented for each plate. In the first position (present study), the plate is attached near the start of heating ($a = 0.25H$); while in the second position (Dutta et al. [4]), baffle is placed at a distance ($a = 6.0H$) from the start of heating. Note that results of Dutta et al. [4] are modified to accommodate differences in the length and velocity scales. Dutta et al. [4] used channel height and channel centerline velocity as reference; whereas, this paper takes channel hydraulic diameter and average velocity as reference. It is found that the heat transfer coefficient profiles shift with the baffle position and upstream of baffles is not significantly affected. In both perforated and solid plates, the presently studied position is better than the previously studied position for this given test configuration.

Figure 10 compares the friction factor ratio with the average Nusselt number ratio for eight different baffle configurations. Like Dutta et al. [4], smooth and ribbed side results of Chandra et al. [12] for a 1 : 2 aspect ratio channel are included for comparison. Note that the aspect ratio of the present work is 2.5 times greater than the ribbed channel [12] and unlike Chandra et al. [12],

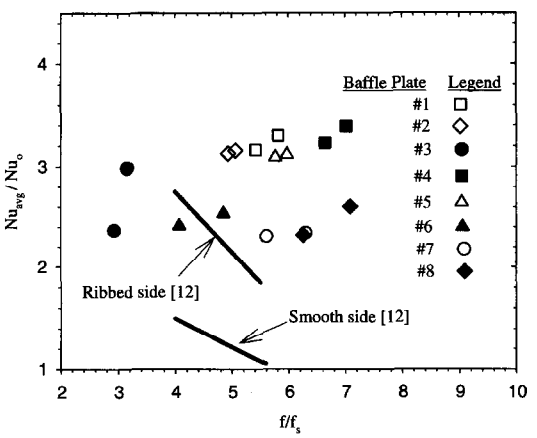

Fig. 10. Qualitative performance comparison of baffles with ribbed channel [12].

present heat transfer results are for centerline only. Kays and Crawford [10] reported that fully developed friction factor and Nusselt number increases with aspect ratio. Friction factors in this high aspect ratio channel for a smooth channel condition is 1.25 times higher than those of Chandra et al. [12]. There are inherent differences in the experimental conditions between this work and Ref. [12]. Therefore, a direct numeric comparison should be avoided between plotted ribbed and baffle data, but a qualitative discussion is feasible. Results indicate that the friction factor can significantly vary with the baffle plate, but the average Nusselt number ratio stays in a closer upper (3.39) and lower (2.32) limits. Unlike the ribbed channel results [12] that show a characteristic drop in the average Nusselt number ratio with an increasing Reynolds number (increasing friction factor ratio), a different pattern is observed for baffle plate. The average Nusselt number ratio stays mostly flat with different Reynolds numbers tested for all baffles, but varies from plate to plate due to differences in porosity and orientation. It can be argued that the ribs cause comparatively smaller scale disturbances than the baffle plates and the effects of ribs on heat transfer enhancement gradually decrease with an increase in the Reynolds number and associated turbulence. Unlike ribs, the baffle plates cause larger scale flow disturbances and the heat transfer coefficient enhancement is equally effective for a large variation in Reynolds number. Another interesting observation is that friction factors with perforated and solid plates are comparable, but heat transfer enhancement by perforated baffles is significantly higher than a solid baffle.

Figure 11 shows that the friction factor reduces dramatically (as expected) with decrease in the angle due to less deflection and less blockage of bulk flow. Table 2 lists the baffle orientations used for this figure. As observed in Fig. 10, Fig. 11 also shows that solid baffles have comparable or higher friction factors but lower heat transfer enhancement capabilities. Heat transfer enhancement by perforated baffles significantly decrease with a decrease in the angle of attack and heat transfer enhancement in the smallest angle for both solid and perforated baffles. Interestingly, the Nusselt number ratio for a solid baffle is less sensitive to the change of angle but the friction factor sensitivity is similar to a perforated baffle. Therefore, it can be argued that the major heat transfer enhancement by perforated baffle is due to jet impingement and major contributor in friction factor ratio is the bulk flow deflection by these baffle plates.

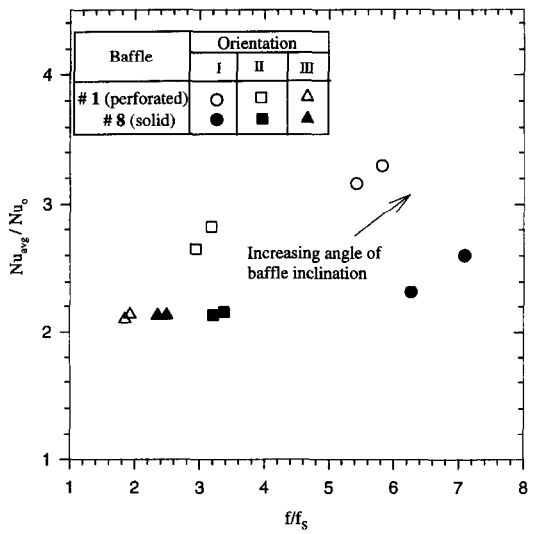

Fig. 11. Variation of Nusselt number ratio with friction factor ratio for a change in the angle of baffle inclination.

4. Conclusions

The main conclusions emerging from this experimental heat transfer and friction factor analysis are as follows:

(a) Inclined perforated baffles can combine the heat transfer enhancement techniques used in ribs, flow inserts, and jet impingement. The perforated density, position, and size of baffles have a significant effect in the internal cooling heat transfer;

(b) Heat transfer characteristics curve shifts with the position of the baffle and the heat transfer coefficient distribution at the upstream of the baffle is mostly unaffected. Dimension of the heat transfer surface determines the optimum position of the baffle;

(c) Both average and local Nusselt numbers are significantly dependent on the baffle plate orientation and the Nusselt number ratio decreases as the plate is placed at a more streamlined position;

(d) The peak heat transfer region occurs at a region covered by the perforated baffle for the configurations studied. Therefore, the perforated baffles may be placed at the high heat flux region for an effective cooling;

(e) The friction factor ratio decreases with a decrease in the angle of baffle and also with an increase in the perforation density. Moreover, friction-factor ratio increases with an increase in the average Nusselt number ratio for a given configuration;

(f) The average Nusselt number ratio mostly stays the same with different Reynolds numbers for a given baffle plate, whereas, ribbed channel shows a decrease in the average Nusselt number ratio with an increase in the Reynolds number.

Acknowledgement

This work is partially supported by Research and Productivity Scholarship offered by SPAR of the Uni-

versity of South Carolina. Their contributions are acknowledged.

References

[1] Incropera FP, DeWitt DP. Fundamentals of Heat and Mass Transfer, 3rd ed. New York: John Wiley and Sons, 1990.

[2] Berner C, Durst F, McEligot DM. Flow Around Baffles. ASME Journal of Heat Transfer 1984;106:743–9.

[3] Habib MA, Mobarak AM, Sallak MA, Abdel Hadi EA, Affify RI. Experimental investigation of heat transfer and flow over baffles of different heights. ASME Journal of Heat Transfer 1984;116:363–8.

[4] Dutta S, Dutta P, Jones RE, Khan JA. Experimental Study of Heat Transfer Coefficient Enhancement with Inclined Solid and Perforated Baffles, International Mechanical Engineering Congress and Exposition, Dallas, Texas, ASME Paper No. 97-WA/HT-4, November 16–21, 1997.

[5] Goldstein RJ, Timmers JF. Visualization of heat transfer from arrays of impinging jets. International Journal of Heat and Mass Transfer 1982;25:1857–68.

[6] Koopman RN, Sparrow EM. Local and average transfer coefficients due to an impinging row of jets. International Journal of Heat and Transfer 1976;19:673–83.

[7] Florschuetz LW, Truman CR, Metzger DE. Streamwise flow and heat transfer distributions for jet array impingement with crossflow. ASME Journal of Heat Transfer 1981; 103:337–42.

[8] Lin ZH, Chou YJ, Hung YH. Heat transfer behavior of a confined slot jet impingement. International Journal of Heat and Mass Transfer 1997;40:1095–107.

[9] Han JC, Heat transfer and friction characteristics in rectangular channels with rib turbulators. ASME Journal of Heat Transfer 1988;110:321–8.

[10] Kays WM, Crawford ME. Convective Heat and Mass Transfer. New York: McGraw-Hill, 1980.

[11] Seyedein SH, Hasan M, Mujumdar AS. Laminar flow and heat transfer from multiple impinging slot jets with an inclined confinement surface. International Journal of Heat and Mass Transfer 1994;37:1867–75.

[12] Chandra PR, Niland ME, Han JC. Turbulent flow heat transfer and friction in a rectangular channel with varying number of ribbed walls. International Gas Turbine and Aeroengine Congress & Exposition, Houston, Texas, ASME Paper No. 95-GT-13, June 5–8, 1995.